HHS Public Access

Author manuscript

Alcohol. Author manuscript; available in PMC 2018 May 01.

Published in final edited form as:

Alcohol. 2017 May ; 60: 115–120. doi:10.1016/j.alcohol.2017.02.176.

Alignment of the Transcriptome with Individual Variation in Animals Selectively Bred for High Drinking-In-the-Dark (HDID)

Robert Hitzemann, **Denesa Oberbeck**, **Ovidiu Iancu**, **Priscila Darakjian**, **Shannon McWeeney**, **Stephanie Spence**, **Jason Schlumbohm**, **Pamela Metten**, and **John Crabbe**

Abstract

Among animals at risk for excessive ethanol consumption such as the HDID selected lines, there is considerable individual variation in the amount of ethanol consumed and the associated blood ethanol concentrations (BECs). For the HDID lines, this variation occurs even though the residual genetic variation associated with the DID phenotype has been largely exhausted and thus is most likely associated with epigenetic factors. Here we focus on the question of whether the genes associated with individual variation in HDID-1 mice are different from those associated with selection (risk) (Iancu et al. 2013). Thirty-three HDID-1 mice were phenotyped for their BECs at the end of a standard DID trial, were sacrificed 3 weeks later and RNA-Seq was used to analyze the striatal transcriptome. The data obtained illustrated that there is considerable overlap of the risk and variation gene sets; both focus on the fine tuning of synaptic plasticity.

Introduction

Although search results are notoriously inaccurately for estimating the true number of citations, it appears relatively safe to conclude that there are now more than 100 publications using genome-wide tools to align the brain transcriptome with some aspect of excessive ethanol consumption. Extensive data are now available for the transcriptional features associated with the risk of developing and/or the consequences of excessive ethanol consumption and withdrawal. The “risk” transcriptome has generally been studied in two contexts: selective breeding or large panels of inbred, including recombinant inbred, strains of mice and rats. Here we focus on one of the HDID selected lines, the HDID-1; this line has been bred for more than 30 generations, using blood ethanol concentrations (BECs) as the selection phenotype. Although the heritability of the HDID phenotype is relatively low (~ 0.1), selection has raised the average BEC at the end of the DID trial to > 1.8 mg/ml. This BEC is 5–6 fold greater than the average BEC obtained in the founder heterogeneous stock animals (HS/NPT) (Barkley-Levenson and Crabbe, 2014; Crabbe et al. 2014). One assumes given the duration of selection that any remaining genetic diversity, relevant to the selection phenotype, would only be found only in genes with very small effect sizes. However, HDID-1 animals continue to exhibit substantial and stable phenotypic variance with BECs frequently ranging from 0.5 to 3.0 mg/ml. This variability could in part be generated by the

residual genetic diversity but it is more likely the result of gene×environment interactions, that have led to stable genome changes e.g. methylation, demethylation and so on.

The first step in understanding this process would be to determine whether one can align transcriptional features with individual variation. A key question to be addressed and the rationale for the present study, was whether or not the genes and/or gene networks associated with individual variation are similar to the genes and gene networks associated with selection. To our knowledge, only Mulligan et al. (2011) have examined features related to DID and individual variation. These authors focused on the relationships between the transcriptome and the individual variation among C57BL/6 inbred mice. Animals were sacrificed at the end of the DID trial so that it was not possible to unravel the predisposition for consumption from the effects of consumption. Nonetheless, these authors detected a strong relationship between the BEC and a striatal network modules enriched in gene annotations for protein binding and oxidative phosphorylation. These data differ from the neuronal membrane related annotations associated with HDID selection (Iancu et al. 2013).

Methods

Animals

S_{27} HDID-1 animals were used in the current study. Details concerning the selection of the HDID animals are found in (Crabbe et al., 2009). The HDID-1 selected line began with a "within family" selection design but was switched to mass selection at S_5. Note the selection phenotype differed from the original DID phenotype reported by Rhodes et al. (2005). All animals were on reversed light-dark cycle. Genotypic details concerning the HDID-1 line are found in Iancu et al. (2013). Animals underwent the standard 4-day DID trial with three 2 hour exposures to a single bottle of 20% ethanol and a final day of 4 hour exposure. The DID trial always began 3 hours into the dark phase. BECs were obtained at the end of the 4^{th} hour as described elsewhere (Crabbe et al. 2009). Eighteen males and 17 females were sacrificed 3 weeks later and used for gene expression analyses. All animals were sacrificed between 10 AM and 2 PM. All animal care, breeding, and testing procedures were approved by the Institutional Animal Care and Use Committees at the Veterans Affairs Medical Center, Portland, OR, and the Oregon Health & Science University, Portland, OR.

Dissection of tissue for gene expression analysis; extraction of RNA

Mice were euthanized, brains removed and immediately frozen on dry ice. Frozen brains were slightly thawed and dissected by hand under RNAse-free conditions. Using the optic chiasm as the rostral marker, a 2 mm coronal slice of brain tissue was isolated. Beginning at the medial ventral aspect of the striatum and recognizing that the striatum has a partial cone shape, the dissection moved dorsal 1 mm, followed by a cut to the lateral boundary of the striatum, with a final cut following the lateral-ventral boundary. The isolated tissue was immediately placed into 1 ml of Trizol (Invitrogen, Carlsbad, CA). Additional details of the RNA extraction and sample preparation are found in Malmanger et al. (2006).

RNA-Seq

Library formation (polyA+, stranded) and sequencing were all performed according to Illumina's specifications at the OHSU Massively Parallel Sequencing Shared Resource. Libraries were multiplexed 6 per lane, yielding approximately 25 to 30 million total reads per sample. FastQC was used for quality checks on the raw sequence data. Sequence data were then aligned using STAR (Spliced Transcripts Alignment to a Reference [Dobin et al. 2013]) allowing for a maximum of three mismatches per 100bp read. For all samples > 85% of the reads uniquely aligned. Using the Bedtools suite, reads were aligned to known genomic features to generate counts at the gene level. Gene expression data were imported into the R application environment; upper-quartile normalization was performed using the edgeR Bioconductor package (Robinson et al. 2010). The read density threshold for inclusion in the data analyses for genes was 30 or approximately 1 count per million reads.

Data Analysis

Sex was confirmed using *Xist* expression. Outlier detection was performed by a combination of manual inspection of individually selected genes as well as a statistical procedure that examines and compares all gene expression levels as described previously (Iancu et al., 2012). In addition, all samples were analyzed to determine if the expected enrichment in striatal genes e.g. *Drd2, Drd1a* and *Rgs9*, over the level of expression in cortical or whole brain samples was detected. The expected enrichment for key markers was > 10-fold. One sample (S5) did not meet criteria; the data were analyzed jointly (males and females). Pearson correlations were used to align gene expression with the BECs. A FDR of ≤ 0.05 (~ $p < 0.01$) was used as the threshold for annotation. The GOrilla algorithm (Eden et al. 2009) was used to detect annotation enrichment. The Enrichr tool set (Chen et al. 2009; Kuleshov et al. 2016) was used to further characterize the affected genes.

Coexpression network construction

We constructed a gene coexpression network utilizing the WGCNA approach (Zhang and Horvath, 2005). The procedure starts by constructing an adjacency matrix on the basis of pairwise Pearson correlations between genes over samples. Next, the adjacency matrix entries are raised to a power β chosen in accordance with the scale-free fit criterion (Zhang and Horvath, 2005). The transformed matrix was clustered using the cutTreeDynamic WGCNA function, resulting in groups of co-expressed genes denoted as modules. Gene connectivity is computed as the sum of all network adjacencies for a given gene; restricting the summation within the gene's own module results in modular connectivity. Connectivity values are reported on a percentile scale and genes in the top 20% are denoted as hubs. Visualization of modules, consumption and annotation results was performed utilizing the Cytoscape software package (Shannon et al. 2003). Additional details are found in Colville et al. (2017).

Results

Individual Variation

Eighteen male and seventeen female animals that were used for the gene expression analyses completed a single 4-day DID trial. The day 4 BECs are illustrated in Figure1. Average BECs +/− SE in the males and females were 1.32 +/− 0.16 and 1.43 +/− 0.21, respectively. Variances in the males and females were not significantly different (F-test; $p > 0.25$).

Gene Expression Analysis

RNA-Seq analysis was performed on striatal samples taken 3 weeks after the DID trial. The data for all Ensembl "gene" annotations (N=42,278) are found in Table S1; of these 14,340 were included in the data analysis (Table S2). One sample (S5) (see Table S1) was identified as an outlier because of unusually low expression in *Drd1, Drd2 and Rgs9*; sample S18 was also identified as an outlier based on statistical procedures (see Methods). Pearson correlations were used to assess the relationships between gene expression and the BEC. 557 genes met the criteria for inclusion in the gene set enrichment analysis (see Methods); the bias was sharply to positive correlations (375 positive versus 182 negative) (Table S3 – highlighted genes). This group of genes, denoted as the "affected gene set" were characterized by two complementary approaches. The first strategy utilized a gene set enrichment analysis strategy to identify GO categories preferentially represented within the affected gene set. The genes positively and negatively correlated to the BEC were analyzed jointly and separately; the most significant (FDR < 0.01) annotation enrichments were for the positively correlated "affected" genes (Table 1). Broadly, the enriched gene categories were associated with the regulation of synaptic function. Genes associated with the category "regulation of synaptic vesicle exocytosis" included *Grik5, Syn1, Stxbp1, Stx1a, Rims4, Rims1* and *Stx1b*. Genes associated with the category "synapse part" included *Camk2g, Chrm3, Crhbp, Gria3, Grin1, Strn4, Syngap1* and *Syt2*. Complete lists of the genes associated with each of the categories are found in Table S4.

The second strategy involved constructing a coexpression network and identifying modules that contain an over-abundance of "affected set" genes. Additionally, examination of modular and network connectivity structure led to the identification of hubs (highly connected genes) that were in the affected gene set and/or in the affected modules. A comprehensive listing of these results is available in Table S3.

The network clustering procedure identified 43 module identified by arbitrary colors; 82 genes did not cluster and were identified as grey. Three modules were significantly enriched in affected genes: black, paleturquoise and turquoise (Table S3). The most significant effect was for the turquoise module (Fisher exact test odds ratio > 5, p value < 10^{-80}). GO annotation for the turquoise module was similar to the annotation for the affected gene set and included numerous categories related to modulation of synaptic function and membrane categories. (Table S4). The enrichment in Component features is illustrated graphically in Figure 2. Key component features included synapse (FDR < 0.1×10^{-7}), and postsynaptic density (FDR < 5×10^{-6}).

For the turquoise module, the overlap with the affected gene set and the annotation structure is illustrated in Figure 3. Enrichment was noted for both positively and negatively correlated genes (red and blue, respectively). The hub genes were enriched in in positively correlated genes while the negative correlated genes had lower intramodular connectivity. (Figure 3A). Hub genes in the turquoise module that were also members of the affected gene set included *Mark1, Syngap1, Strn4, Gria3*, and *Dclk1*.

Further Characteristics of Affected Gene Set

The Enrichr tool set (see Methods) was used to further characterize the affected gene set. The analysis for the TRANSFAC and JASPAR position weighted matrix scores (PWMs) revealed a significant enrichment in binding sites associated with several transcription factors including transcriptional enhancer domain family member 2 (TEAD2) ($p < 3\times10^{-14}$), early growth response 1 (EGR1) ($p < 7\times10^{-11}$), specificity protein 1 (SP1) ($p < 3\times10^{-10}$), signaling effectors mothers against decapentaplegic protein 4 (SMAD4) ($p < 2\times10^{-9}$) and nuclear factor kappa beta 1 (NFKB1)($p < 2\times10^{-9}$). The genes associated with each of these transcription factors are found in Table S5. None of these transcription factors were in the affected gene set. No significant enrichments in miRNA binding sites were detected among the affected genes, although there were trends for enrichment in MIR-296,-33 and -374 ($p > 0.13$).

The top ten protein-protein-interaction hub proteins were identified (Table S6). *Ywab* encodes for 14-3- 3β which interacts with 51 members of the affected gene set ($p < 2\times10^{-18}$) (Table S6). *Dlg4* (discs large homolog 4) encodes for postsynaptic density protein 95 (PSD-95); this hub interacts with 31 members of the affected gene set.

Discussion

Numerous studies, QTL, GWAS and transcriptomics, have focused on mapping the genes associated with the increased *risk* for excessive ethanol consumption (see e.g. Mulligan et al. 2006; Kendler et al. 2013; Contet 2012; Saba et al. 2015; Iancu et al. 2013; Metten et al. 2014). Genes associated with signal transduction (especially Ras-MAPK-ERK pathways), synaptic plasticity, neuroimmune function, cell growth and transcription have been frequently detected. Iancu et al. (2013) used microarray-based strategies to compare the genotypes and striatal transcriptomes of the HDID-1 and HDID-2 selected lines and the HS/NPT founders. The genotype data revealed as expected a significantly reduced genetic complexity in the selected lines compared to the founders but also illustrated that the selected lines were different, consistent with the differences in the patterns of ethanol consumption (Barkley-Levenson and Crabbe, 2015). . The common QTLs detected for both selections did not overlap with known QTLs for ethanol preference (see e.g. Metten et al. 2014). The analysis of the gene expression data focused on a network-based strategy (Zhang and Horvath, 2005) to detect gene modules and hub nodes that were strongly affected by selection. Two of the network modules were significantly affected by selection: black and magenta. Module sizes were 148 and 265 genes, respectively; total genes in the consensus selection network were 7.380. We asked whether there were significant overlaps between the genes in these modules and the affected gene set detected in the current study.

There was no significant overlap with the magenta module but there was overlap (60/475) with the black module ($p < 2\times10^{-10}$) (See Table S7). Annotation for the black module is also found in Table S7. Note the marked enrichments in annotations associated glutamate secretion, neurological system process, synaptic vesicle, plasma membrane part and the synapse. These annotations are similar to and in some cases overlap with the annotations reported in Table S4 for the affected gene set and/or the turquoise module. Thus, we conclude, at least from a broad perspective, that there is an overlap in terms of process and component for the genes associated with selection (*risk*) and the genes mediating individual variation in the DID model. It also should be noted that while there was no significant overlap with the genes in the magenta module, there was a significant overlap in terms of annotation e.g. postsynaptic density. The genes in the magenta module (Iancu et al. 2013) associated with related postsynaptic categories included *Camk2n1, Dlgap2, Dlgap3, Faim2, Gabrg1, Glra2, Grik1, Homer1, Lin7b* and *Neto1*. Thus, while the genes are different, both sets of genes are involved in the fine tuning of synaptic activity. Further, there is ample evidence that the risk and individual variation genes interact e.g. *Dlgap2* and *Dlg4* (see e.g. Hirao et al. 1998).

Within the black module found in Iancu et al. (2013), *Dgkz* emerged as a key hub node associated with selection; intramodular connectivity increased in both selected lines such that *Dgkz* moved from non-hub to hub status. This was viewed as potentially important since *Dgkz* has potential behavioral links. For example, Kim and colleagues (2009) have shown that the synaptic removal of diacylglycerol by DGKzeta and PSD-95 regulates synaptic spine maintenance. Chronic EtOH exposure has been shown to affect spine density and/or morphology (Carpenter-Hyland and Chandler, 2006; Zhou et al., 2007). Further, in comparison with EtOH-avoiding NP rats, EtOH-preferring P rats have a lower dendritic spine density in the amygdala (Moonat et al., 2011). In the current study *Dgkz* is a member of the affected gene and is a member with moderate connectivity of the turquoise module; *Dlg4*, which encodes for PSD-95 is a strong hub in the turquoise module and was identified as a protein-protein interaction hub for the affected gene set. The key role of PSD-95 is regulating synaptic plasticity at NMDA –mediated synapses will not be reviewed here. However, it should be noted that *Grin1* was also a member of the affected gene set. PSD-95 has been found to have key role in regulating ethanol intoxication and consumption. For example, Camp et al. (2012) found in PSD-95 KO mice, the sedative/hypnotic effects of ethanol were enhanced but ethanol consumption was decreased, especially at higher concentrations, under free access conditions. There is also ample evidence that PSD-95 has a key role in the synaptic plasticity associated with chronic ethanol intoxication and ethanol tolerance (e.g. Daut et al. 2015; Maiya et al. 2012).

We note one additional similarity between the genes associated with risk and individual variation, the involvement of calcium/calmodulin-dependent type II protein kinases. *Camk2a, Camk2b, Camk2c* and *Camkk2* were found in the affected gene set and/or within the turquoise module in the current study. Both *Camkk2* and *Camk2n1* are members of the magenta module in the Iancu et al. (2013) study (see above) where they were found to be strongly affected by selection. Collectively, these data reinforce the likely importance that CAM kinases have in modulating ethanol consumption (see e.g. Easton et al. 2013).

This special issue of the Journal focuses on alcohol and epigenetic mechanisms. As many of the associated articles have reported, acute, chronic and intermittent exposures to alcohol have substantial epigenetic effects (see e.g. Berkel and Pandey 2017; Lopez-Moreno et al. 2015). While the breadth of epigenetic changes in synaptic function remain to be completely determined, changes in genes e.g. NR2B, associated with synaptic plasticity have been detected (Qiang et al. 2011), The intent of the data presented here was to identify another area of potential epigenetic interest, namely the substantial individual variation in ethanol consumption among animals at a high risk for excessive consumption, the HDID-1. This variation is seen not only in the selected line but also among inbred mouse strains such as the C57BL/6J which consume excessive amounts of alcohol in both free and limited access conditions (e.g. Mulligan et al. 2011). Given the stability of the variation, one is led to speculate that epigenetic mechanisms are involved. Similarly Wolstenholme et al. (2011) concluded that epigenetic mechanisms account, in part, for the individual variation among C57BL/6J mice in 2-bottle choice consumption. However, we recognize that mechanisms not related to epigenetic factors may influence individual variation. For example, the wide variation among individuals in striatal *Drd2* expression seen in this study and elsewhere (e.g. Hitzemann et al. 2003) is not correlated with the expression of “epigenetic” related genes but has marked behavioral consequences (Hitzemann et al. 1995). Understanding the causes of such variation will be key to developing new therapeutic strategies for the treatment of alcoholism and other drugs of abuse.

Supplementary Material

Refer to Web version on PubMed Central for supplementary material.

Acknowledgments

This study was supported in part by grants AA13484, AA13519, AA20245

References

Barkley-Levenson AM, Crabbe JC. High drinking in the dark mice: a genetic model of drinking to intoxication. Alcohol (Fayetteville, N.Y.). 2014; 48(3):217–223. https://doi.org/10.1016/j.alcohol.2013.10.007.

Berkel, TDM., Pandey, SC. Emerging role of epigenetic mechanisms in alcohol addiction. Alcohol Clin Exp Res. 2017. Accepted Author Manuscript. http://dx.doi.org/10.1111/acer.13338

Camp MC, Feyder M, Ihne J, Palachick B, Hurd B, Karlsson R-M, Noronha B, Chen YC, Coba MP, Grant SG, Holmes A. A novel role for PSD-95 in mediating ethanol intoxication, drinking and place preference. Addiction Biology. 2011; 16(3):428–439. https://doi.org/10.1111/j.1369-1600.2010.00282.x. [PubMed: 21309945]

Carpenter-Hyland EP, Chandler LJ. Homeostatic plasticity during alcohol exposure promotes enlargement of dendritic spines. The European Journal of Neuroscience. 2006; 24(12):3496–3506. https://doi.org/10.1111/j.1460-9568.2006.05247.x. [PubMed: 17229098]

Chen G, Reilly MT, Kozell LB, Hitzemann R, Buck KJ. Differential activation of limbic circuitry associated with chronic ethanol withdrawal in DBA/2J and C57BL/6J mice. Alcohol (Fayetteville, N.Y.). 2009; 43(6):411–420. https://doi.org/10.1016/j.alcohol.2009.05.003.

Colville, AM., Iancu, OD., Oberbeck, DL., Darakjian, P., Zheng, CL., Walter, NAR., Harrington, CA., Searles, RP., McWeeney, S., Hitzemann, RJ. Effects of selection for ethanol preference on gene expression in the nucleus accumbens of HS-CC mice. Genes, Brain and Behavior. 2017. (Accepted Author Manuscript). http://dx.doi.org/10.1111/gbb.12367

Contet C. Gene Expression Under the Influence: Transcriptional Profiling of Ethanol in the Brain. Current Psychopharmacology. 2012; 1(4):301–314. [PubMed: 24078902]

Crabbe JC, Metten P, Rhodes JS, Yu CH, Brown LL, Phillips TJ, Finn DA. A line of mice selected for high blood ethanol concentrations shows drinking in the dark to intoxication. Biological Psychiatry. 2009; 65(8):662–670. https://doi.org/10.1016/j.biopsych.2008.11.002. [PubMed: 19095222]

Crabbe, JC. Neurobiology of Alcohol Dependence. San Diego: Academic; 2014. Chapter 18 - The Genetic Complexity of Alcohol Drinking in Rodents; p. 359-375.http://www.sciencedirect.com/science/article/pii/B9780124059412000183

Daut RA, Busch EF, Ihne J, Fisher D, Mishina M, Grant SGN, Camp M, Holmes A. Tolerance to ethanol intoxication after chronic ethanol: role of GluN2A and PSD-95. Addiction Biology. 2015; 20(2):259–262. https://doi.org/10.1111/adb.12110. [PubMed: 24397780]

Dobin A, Davis CA, Schlesinger F, Drenkow J, Zaleski C, Jha S, Batut P, Chaisson M, Gingeras TR. STAR: ultrafast universal RNA-seq aligner. Bioinformatics (Oxford, England). 2013; 29(1):15–21. https://doi.org/10.1093/bioinformatics/bts635.

Easton AC, Lucchesi W, Lourdusamy A, Lenz B, Solati J, Golub Y, Lewczuk P, Fernandes C, Desrivieres S, Dawirs RR, Moll GH, Kornhuber J, Frank J, Hoffmann P, Soyka M, Kiefer F, The GESGA Consortium. Schumann G, Giese KP, Muller CP. αCaMKII autophosphorylation controls the establishment of alcohol drinking behavior. Neuropsychopharmacology. 2013; 38(9):1636–1647. https://doi.org/10.1038/npp.2013.60. [PubMed: 23459588]

Eden E, Navon R, Steinfeld I, Lipson D, Yakhini Z. GOrilla: a tool for discovery and visualization of enriched GO terms in ranked gene lists. BMC Bioinformatics. 2009; 10:48. https://doi.org/10.1186/1471-2105-10-48. [PubMed: 19192299]

Hirao K, Hata Y, Ide N, Takeuchi M, Irie M, Yao I, Deguchi M, Toyoda A, Sudhof TC, Takai Y. A novel multiple PDZ domain-containing molecule interacting with N-methyl-D-aspartate receptors and neuronal cell adhesion proteins. The Journal of Biological Chemistry. 1998; 273(33):21105–21110. [PubMed: 9694864]

Hitzemann R, Qian Y, Kanes S, Dains K, Hitzemann B. Genetics and the organization of the basal ganglia. Int Rev Neurobiol. 1995; 38:43–94. [PubMed: 8537205]

Hitzemann R, Hitzemann B, Rivera S, Gatley J, Thanos P, Shou LL, Williams RW. Dopamine D2 receptor binding, Drd2 expression and the number of dopamine neurons in the BXD recombinant inbred series: genetic relationships to alcohol and other drug associated phenotypes. Alcoholism, Clinical and Experimental Research. 2003; 27(1):1–11.

Iancu OD, Darakjian P, Malmanger B, Walter NA, McWeeney S, Hitzemann R. Gene networks and haloperidol-induced catalepsy. Genes Brain Behavior. 2012; 1(11):29–37. http://dx.doi.org/10.1111/j.1601-183X.2011.00736.x.

Iancu OD, Oberbeck D, Darakjian P, Metten P, McWeeney S, Crabbe JC, Hitzemann R. Selection for Drinking in the Dark Alters Brain Gene Coexpression Networks. Alcoholism, Clinical and Experimental Research. 2013; 37(8):1295–1303. https://doi.org/10.1111/acer.12100.

Kendler KS, Aggen SH, Prescott CA, Crabbe J, Neale MC. Evidence for multiple genetic factors underlying the DSM-IV criteria for alcohol dependence. Molecular Psychiatry. 2012; 17(12):1306–1315. https://doi.org/10.1038/mp.2011.153. [PubMed: 22105626]

Kim K, Yang J, Zhong X-P, Kim M-H, Kim YS, Lee HW, Seungnam H, Choi J, Han K, Seo J, Prescott SM, Topham MK, Bae YC, Koretzky G, Choi SY, Kim E. Synaptic removal of diacylglycerol by DGKzeta and PSD-95 regulates dendritic spine maintenance. The EMBO Journal. 2009; 28(8):1170–1179. https://doi.org/10.1038/emboj.2009.44. [PubMed: 19229292]

Kuleshov MV, Jones MR, Rouillard AD, Fernandez NF, Duan Q, Wang Z, Koplev S, Jenkins SL, Jagodnik KM, Lachmann A, McDermott MG, Monteiro CD, Gundersen GW, Ma'ayan A. Enrichr: a comprehensive gene set enrichment analysis web server 2016 update. Nucleic Acids Research. 2016; 44(W1):W90–97. https://doi.org/10.1093/nar/gkw377. [PubMed: 27141961]

López-Moreno JA, Marcos M, Calleja-Conde J, Echeverry-Alzate V, Bühler KM, Costa-Alba P, Bernardo E, Laso F-J, Rodríguez de Fonseca F, Nadal R, Viveros MP, Maldonado R, Giné E. Histone Deacetylase Gene Expression Following Binge Alcohol Consumption in Rats and Humans. Alcohol Clin Exp Res. 2015; 39:1939–1950. http://dx.doi.org/10.1111/acer.12850. [PubMed: 26365275]

Maiya R, Lee S, Berger KH, Kong EC, Slawson JB, Griffith LC, Takamiya K, Huganir RL, Margolis B, Heberlein U. DlgS97/SAP97, a neuronal isoform of discs large, regulates ethanol tolerance. PloS One. 2012; 7(11):e48967. https://doi.org/10.1371/journal.pone.0048967. [PubMed: 23145041]

Malmanger B, Lawler M, Coulombe S, Murray R, Cooper S, Polyakov Y, Belknap J, Hitzemann R. Further studies on using multiple-cross mapping (MCM) to map quantitative trait loci. Mammalian Genome: Official Journal of the International Mammalian Genome Society. 2006; 17(12):1193–1204. https://doi.org/10.1007/s00335-006-0070-2. [PubMed: 17143586]

Metten P, Iancu OD, Spence SE, Walter NAR, Oberbeck DL, Harrington CA, Colville A, McWeeney S, Phillips TJ, Buck KJ, Crabbe JC, Belknap JK, Hitzemann RJ. Dual-trait selection for ethanol consumption and withdrawal: genetic and transcriptional network effects. Alcoholism, Clinical and Experimental Research. 2014; 38(12):2915–2924. https://doi.org/10.1111/acer.12574.

Moonat S, Sakharkar AJ, Zhang H, Pandey SC. The role of amygdaloid brain-derived neurotrophic factor, activity-regulated cytoskeleton-associated protein and dendritic spines in anxiety and alcoholism. Addiction Biology. 2011; 16(2):238–250. https://doi.org/10.1111/j.1369-1600.2010.00275.x. [PubMed: 21182574]

Mulligan MK, Ponomarev I, Hitzemann RJ, Belknap JK, Tabakoff B, Harris RA, Crabbe JC, Blednov YA, Grahame NJ, Phillips TJ, Finn DA, Hoffman PL, Iver VR, Koob GF, Bergeson SE. Toward understanding the genetics of alcohol drinking through transcriptome meta-analysis. Proceedings of the National Academy of Sciences of the United States of America. 2006; 103(16):6368–6373. https://doi.org/10.1073/pnas.0510188103. [PubMed: 16618939]

Mulligan MK, Rhodes JS, Crabbe JC, Mayfield RD, Harris RA, Ponomarev I. Molecular profiles of drinking alcohol to intoxication in C57BL/6J mice. Alcoholism, Clinical and Experimental Research. 2011; 35(4):659–670. https://doi.org/10.1111/j.1530-0277.2010.01384.x.

Qiang M 1, Denny A, Lieu M, Carreon S, Li J. Histone H3K9 modifications are a local chromatin event involved in ethanol-induced neuroadaptation of the NR2B gene. Epigenetics. 2011; 6(9):1095–104. http://dx.doi.org/10.4161/epi.6.9.16924. [PubMed: 21814037]

Rhodes JS, Best K, Belknap JK, Finn DA, Crabbe JC. Evaluation of a simple model of ethanol drinking to intoxication in C57BL/6J mice. Physiol Behav. 2005; 84(1):53–63. [PubMed: 15642607]

Robinson MD, McCarthy DJ, Smyth GK. edgeR: a Bioconductor package for differential expression analysis of digital gene expression data. Bioinformatics (Oxford, England). 2010; 26(1):139–140. https://doi.org/10.1093/bioinformatics/btp616.

Saba LM, Flink SC, Vanderlinden LA, Israel Y, Tampier L, Colombo G, Kiianmaa K, Bell RL, Printz MP, Flodman P, Koob G, Richardson HN, Lombardo J, Hoffman PL, Tabakoff B. The sequenced rat brain transcriptome--its use in identifying networks predisposing alcohol consumption. The FEBS Journal. 2015; 282(18):3556–3578. https://doi.org/10.1111/febs.13358. [PubMed: 26183165]

Shannon P, Markiel A, Ozier O, Baliga NS, Wang JT, Ramage D, Amin N, Schwikowski B, Ideker T. Cytoscape: a software environment for integrated models of biomolecular interaction networks. Genome Research. 2003; 13(11):2498–2504. http://doi.org/10.1101/gr.1239303. [PubMed: 14597658]

Wolstenholme JT, Warner JA, Capparuccini MI, Archer KJ, Shelton KL, Miles MF. Genomic analysis of individual differences in ethanol drinking: evidence for non-genetic factors in C57BL/6 mice. PLoS One. 2011; 6(6):e21100. http://dx.doi.org/10.1371/journal.pone.0021100. [PubMed: 21698166]

Zhang B, Horvath S. A general framework for weighted gene co-expression network analysis. Statistical Applications in Genetics and Molecular Biology. 2005; 4 Article17. https://doi.org/10.2202/1544-6115.1128.

Zhou FC, Anthony B, Dunn KW, Lindquist W, Brent, Xu Z, Deng P. Chronic Alcohol Drinking Alters Neuronal Dendritic Spines in the Brain Reward Center Nucleus Accumbens. Brain Research. 2007; 1134(1):148–161. http://doi.org/10.1016/j.brainres.2006.11.046. [PubMed: 17198693]

- There is considerable individual difference seen in the amount of ethanol consumed in High Drinking in the Dark mice.
- This variation is most likely associated with epigenetic factors.
- There is considerable overlap seen in genes associated with this variation and genes associated with selection (risk) for developing excessive ethanol consumption.
- Many of these genes are related to NMDA-mediated synaptic plasticity.

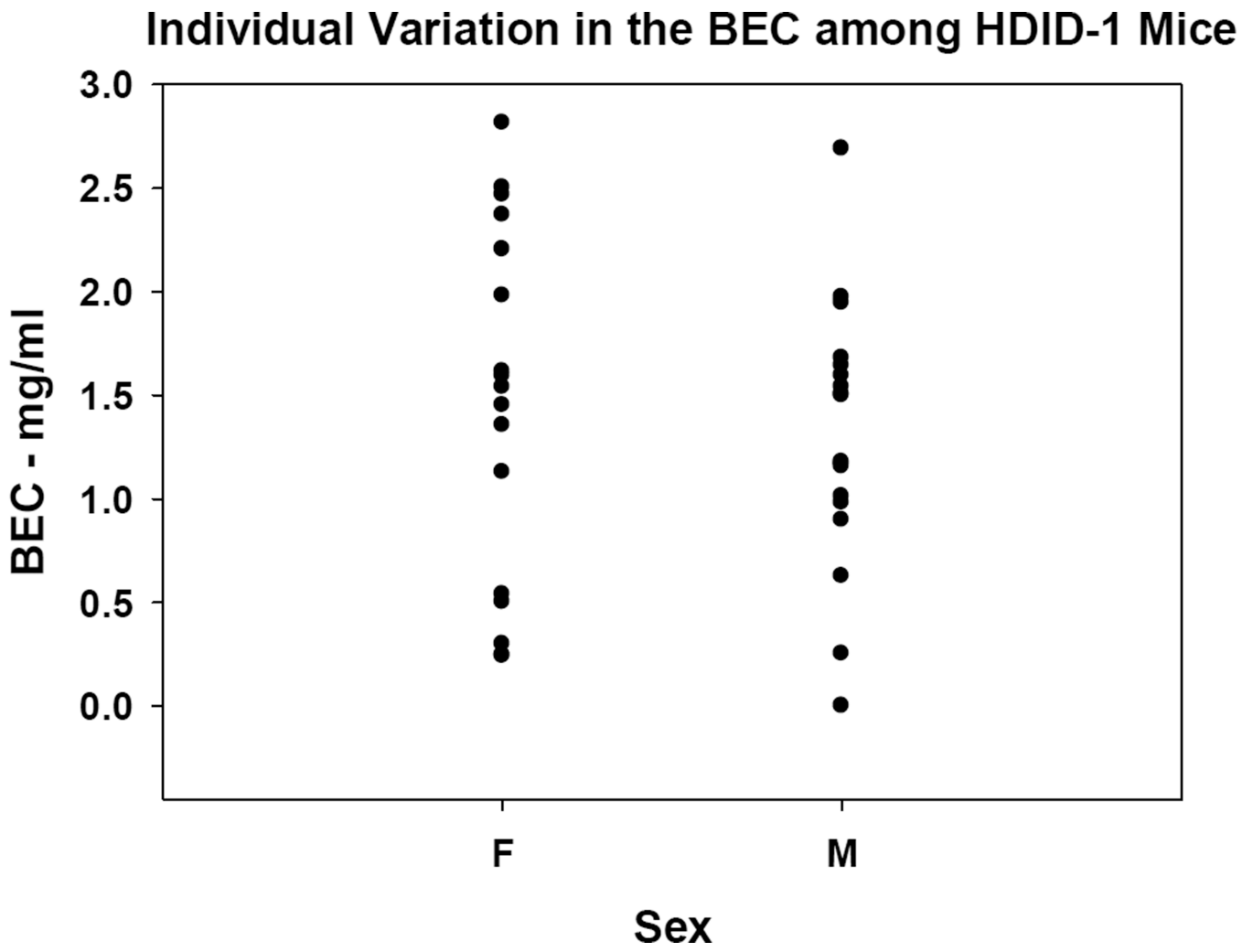

Figure 1. Individual Variation in the BEC among the Male and Female HDID-1 Mice Used for Gene Expression Analysis

Details are similar to those in the legend for figure 1, except that the animals were tested only once. Three weeks later the animals were sacrificed, brains removed and the striatum dissected for RNA-Seq, No significant difference was detected in the variance between the males and females (F-test; $p > 0.25$).

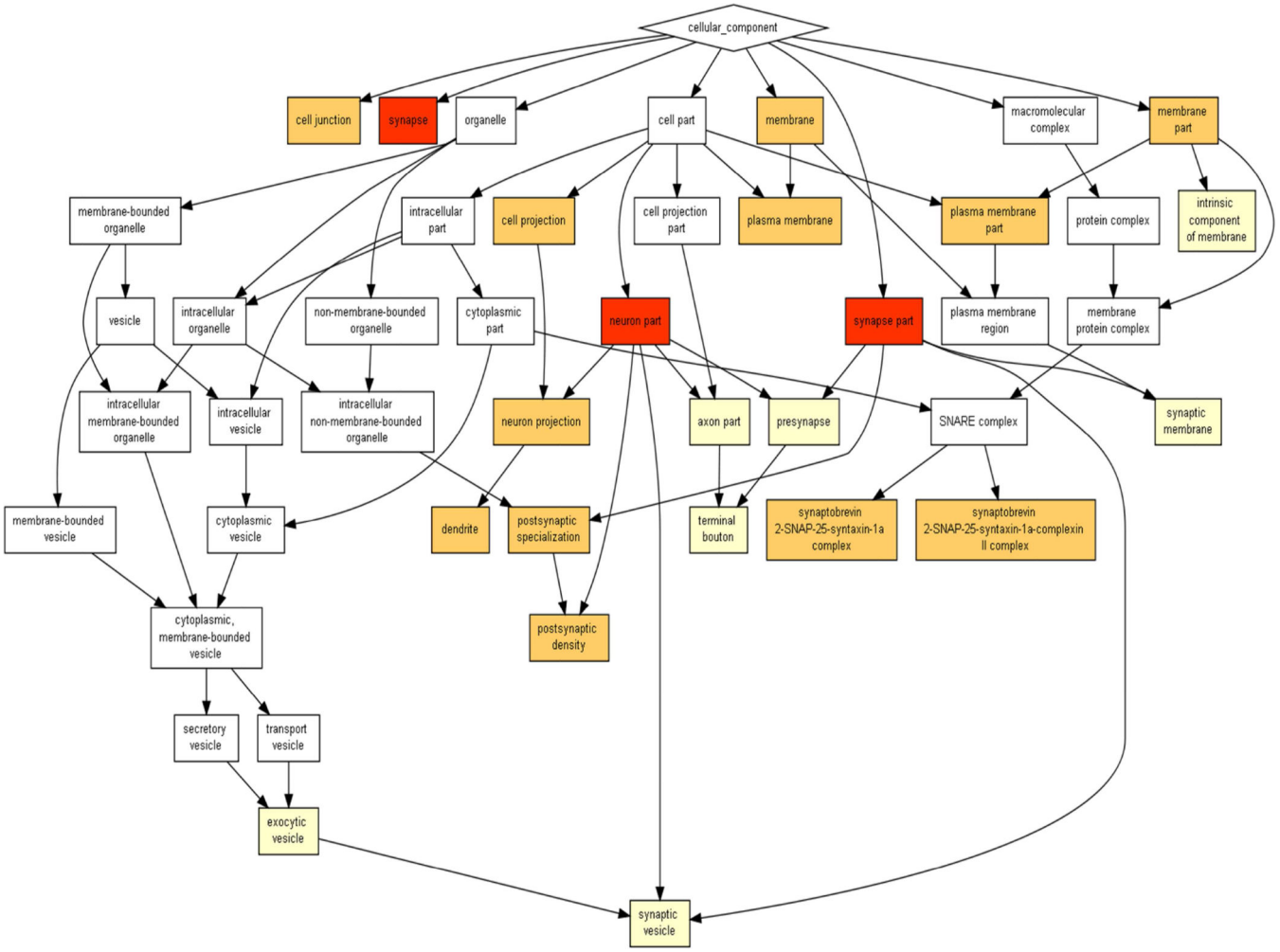

Figure 2. Graphical Representation of the GO Component Annotation Structure for the Affected Gene Set

The boxes are color-coded for significance. Details in Table S4.

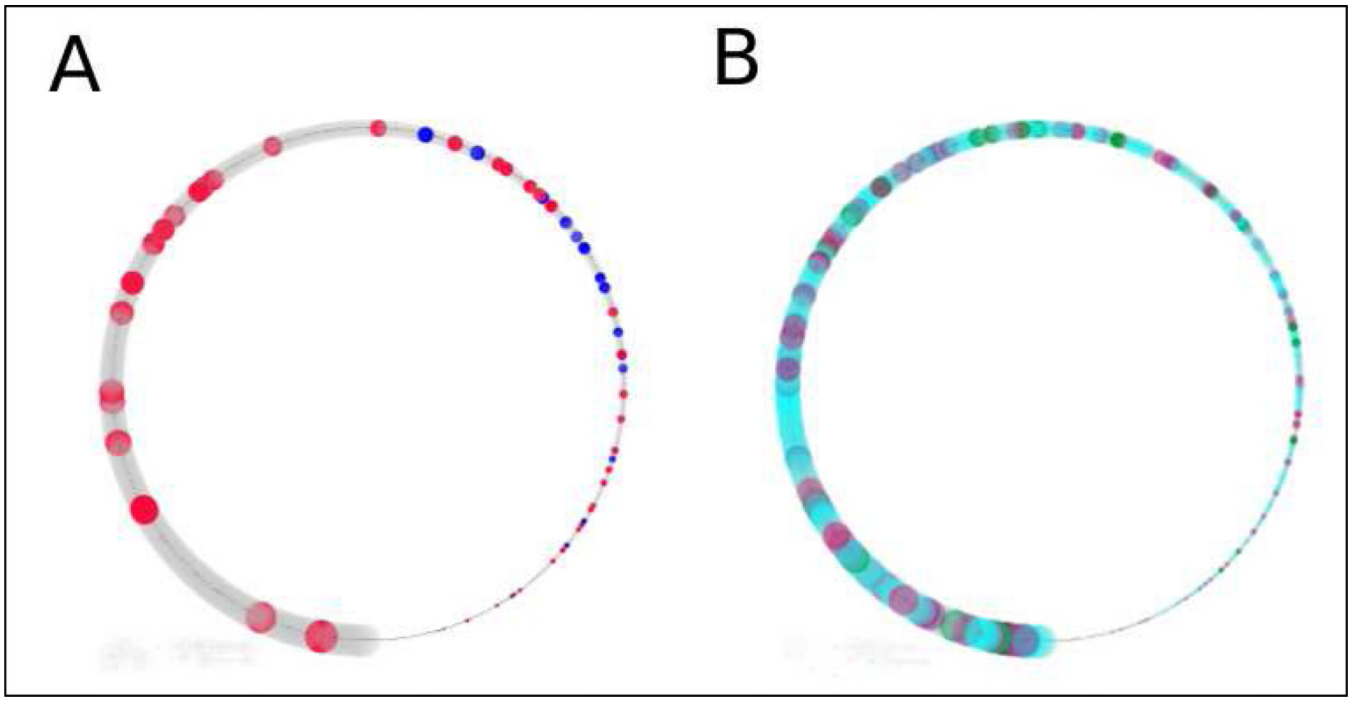

Figure 3. Correlations between consumption and genes in the turquoise coexpression module

A: Positively (red) and negatively (blue) correlated genes. B: Genes annotated with synapse part are colored in cyan, genes annotated with membrane part are colored in green, and genes with both annotations are colored in purple. Node size is proportional to turquoise module connectivity.

Table 1

Enrichment in GO Annotations for Genes Positively Correlated with the BECs in the HDID-1 Selected Line.

GO Term	Description	P-value	FDR q-value	Enrichment[1]
GO Process				
GO:0023061	signal release	2.28E-08	3.09E-04	5.23
GO:2000300	regulation of synaptic vesicle exocytosis	8.43E-07	5.71E-03	12.3
GO:0017158	regulation of calcium ion-dependent exocytosis	8.84E-07	4.00E-03	7.24
GO:0051046	regulation of secretion	1.50E-06	5.07E-03	2.56
GO:1902803	regulation of synaptic vesicle transport	1.59E-06	4.31E-03	9.23
GO:0006904	vesicle docking involved in exocytosis	1.59E-06	3.59E-03	9.23
GO:0046928	regulation of neurotransmitter secretion	1.76E-06	3.41E-03	7.72
GO:0099643	signal release from synapse	2.20E-06	3.73E-03	5.34
GO:0099531	presynaptic process involved in chemical synaptic transmission	2.26E-06	3.40E-03	4.9
GO:1903530	regulation of secretion by cell	3.14E-06	4.25E-03	2.57
GO:0001505	regulation of neurotransmitter levels	6.42E-06	7.92E-03	4.17
GO:1903305	regulation of regulated secretory pathway	7.50E-06	8.48E-03	5.2
GO:1901096	regulation of autophagosome maturation	7.61E-06	7.93E-03	24.6
GO:0007610	behavior	1.08E-05	1.05E-02	2.45
GO:0051588	regulation of neurotransmitter transport	1.09E-05	9.87E-03	6.27
GO:0046903	secretion	1.13E-05	9.61E-03	2.05
GO:0050804	modulation of synaptic transmission	1.27E-05	1.02E-02	2.99
GO:0007269	neurotransmitter secretion	1.28E-05	9.63E-03	6.15
GO:0006836	neurotransmitter transport	1.38E-05	9.85E-03	4.89
GO Component				
GO:0044456	synapse part	4.56E-11	7.75E-08	2.92
GO:0097458	neuron part	7.04E-10	5.98E-07	2.2
GO:0044459	plasma membrane part	2.45E-09	1.39E-06	1.87
GO:0044425	membrane part	3.92E-09	1.66E-06	1.45
GO:0098590	plasma membrane region	3.58E-07	1.22E-04	2.3
GO:0043005	neuron projection	1.22E-06	3.45E-04	2.25
GO:0097060	synaptic membrane	3.16E-06	7.67E-04	3.16
GO:0031224	intrinsic component of membrane	1.87E-05	3.97E-03	1.41
GO:0016020	membrane	2.57E-05	4.85E-03	1.25
GO:0042995	cell projection	3.14E-05	5.34E-03	1.76
GO:0099572	postsynaptic specialization	4.57E-05	7.05E-03	3.17
GO:0014069	postsynaptic density	4.57E-05	6.46E-03	3.17
GO:0048786	presynaptic active zone	5.50E-05	7.19E-03	8.52
GO:0031226	intrinsic component of plasma membrane	5.96E-05	7.23E-03	1.84
GO:0048787	presynaptic active zone membrane	7.73E-05	8.75E-03	27.68
GO:0005886	plasma membrane	9.33E-05	9.91E-03	1.41

[1] Enrichment was calculated using the Gorilla algorithm (Eden et al. (2009). The positively correlated genes (N = were compared to the genes (N=14340) entered into the data analysis (Table S2).